ChemComm

Accepted Manuscript

This is an *Accepted Manuscript*, which has been through the Royal Society of Chemistry peer review process and has been accepted for publication.

Accepted Manuscripts are published online shortly after acceptance, before technical editing, formatting and proof reading. Using this free service, authors can make their results available to the community, in citable form, before we publish the edited article. We will replace this *Accepted Manuscript* with the edited and formatted *Advance Article* as soon as it is available.

You can find more information about *Accepted Manuscripts* in the **Information for Authors**.

ROYAL SOCIETY OF CHEMISTRY

www.rsc.org/chemcomm

Please do not adjust margins

ChemComm

Journal Name

COMMUNICATION

All inorganic cesium lead halide perovskite nanocrystals for photodetector applications

Parthiban Ramasamy,[a,†] Da-Hye Lim,[a,†] Bumjin Kim,[a] Seung-Ho Lee,[a] Min-Sang Lee[b] and Jong-Soo Lee*[a]

We describe a simple, fast and reproducible halide ion exchange reactions in CsPbX$_3$ (X = Cl, Br, I) nanocrystals (NCs) at room temperature. Through the simple adjustment of halide ion concentration, the photoluminescence of these NCs can be tuned over the entire visible region (425-655 nm). Photodetector devices based on all inorganic CsPbI$_3$ NCs have been demonstrated for the first time. The photodetectors exhibited good on/off photocurrent ratio of 10^5.

Recently, hybrid organic-inorganic lead halide perovskites (CH$_3$NH$_3$PbX$_3$, where X = Cl, Br, I) have attracted great attention as light absorbers in photovoltaics due to their amazingly rapid rise in their performance.[1-3] Besides photovoltaics, these perovskites have also been explored as potential in other applications such as water splitting, light-emitting diodes and photodetectors.[4-10] Another potentially attractive but less explored perovskites are all inorganic cesium lead/tin halides (CsPb(Sn)X$_3$, where X = Cl, Br, I). CsSnI$_3$ has been reported to possess excellent hole transport properties in solid state dye-sensitized solar cells.[11] More recently solar cells fabricated using CsPbBr$_3$ as light absorber material showed comparable performances with the organic one (CH$_3$NH$_3$PbBr$_3$), especially in producing high open circuit voltages that are characteristics of perovskite solar cells.[12] Most of the investigations on CsPb(Sn)X$_3$ perovskites have focused on bulk crystals or thin films until Protesescu *et al.* reported a new synthetic method to produce colloidal CsPbX$_3$ nanocrystals earlier this year.[13-16] The CsPbX$_3$ NCs exhibited bright luminescence with quantum yields up to 90% and narrow emission wavelengths that were tuned over the entire visible region depending on the NCs size and halide ions composition.[16] This prompted materials scientists to utilize these NCs for various optoelectronic applications. Amplified

spontaneous emission and tunable electroluminescence have recently been demonstrated from these NCs.[17-19]

Post synthetic transformation reactions in NCs such as cation and anion exchange reactions have emerged as powerful tools for fine control over the NCs composition. Very recently, anion exchange reactions in CsPbX$_3$ NCs have demonstrated to tune the optical properties.[20,21] The growing interest in perovskite nanocrystals motivated us to develope alternative methods for the synthesis of CsPbX$_3$ nanocrystals with tunable optical properties to utilize in optoelectronics.

In this communication, we report facile halide exchange reactions in CsPbBr$_3$ perovskite colloidal NCs and their application in photodetectors for the first time. Halide exchange reaction were carried out at room temperature using lithium salts (LiX, X= I, Cl, Br). The green emission (508 nm) from CsPbBr$_3$ NCs was tuned over the entire visible spectral region (425 - 655 nm) using LiI or LiCl. The halide exchange reactions were found to be very fast and completed within seconds. In addition, photodetectors were fabricated using all inorganic CsPbI$_3$ nanocrystals for the first time.

We chose CsPbBr$_3$ NCs to study the halide exchange reactions, since it has visible green emission around 508 nm which can be tuned either in blue or red side of the visible spectrum by substituting Br$^-$ with Cl$^-$ or I$^-$ ions. The schematic of the exchange reactions is shown in Fig. 1.
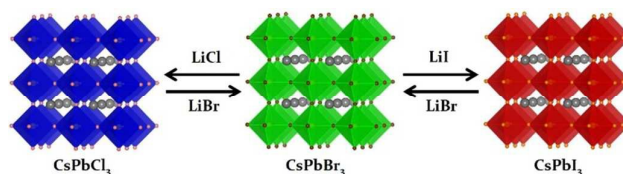

Fig. 1 Schematic of the anion exchange reactions in CsPbX$_3$ NCs.

[a.] Department of Energy Systems Engineering, DGIST, Daegu, 711-873, Republic of Korea. E-mail: jslee@dgist.ac.kr
[b.] Ecolumy Co., Ltd. University-Industry Cooperation Center, DGIST, Daegu, 711-873, Republic of Korea.
† These authors contributed equally

Please do not adjust margins

CsPbBr$_3$ NCs of size around 8 nm were synthesized following the procedure reported by Protesescu et al.[16] The exchange reactions were carried out at room temperature by adding calculated amount of ethanol solution of LiI or LiCl to the CsPbBr$_3$ NCs in hexane. Then the mixtures were shaken vigorously which produced a color change from green to red for LiI and colorless for LiCl. The whole exchange reaction was completed in less than 5 seconds.
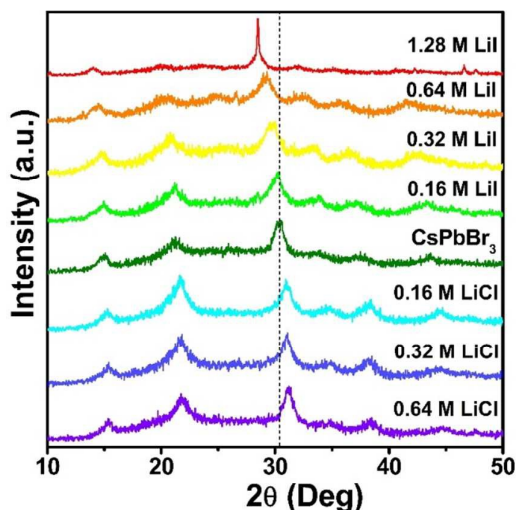

Fig. 2 (a) XRD patterns of the CsPbBr$_3$ NCs exchanged with different concentrations of LiI and LiCl.

As shown in Fig. 2, the as-synthesized CsPbBr$_3$ NCs has a cubic structure (JCPDS No. 54-0752) and remained unaltered after exchanged with I$^-$ or Cl$^-$ anions. However, the (200) reflection at 30.68° gradually shifted to lower angles for Br$^-$ to I$^-$ exchange due to the lattice expansion by substituting larger I$^-$ ion for smaller Br$^-$ ion. In the same manner, the (200) reflection shifted to higher angles for Br$^-$ to Cl$^-$ exchange, in accordance with the lattice contraction. We also observed a change in the intensity of the XRD peaks. For the iodide exchanged samples the intensity of the (200) plane was very high compared with other planes. This shows that the CsPbI$_3$ NCs were grown along the (200) plane direction after the iodide exchange reaction. The morphology of the as-synthesized CsPbBr$_3$ NCs and halide exchange synthesized CsPbI$_3$ and CsPbCl$_3$ NCs were analyzed using transmission electron microscopy (TEM). Both the CsPbCl$_3$ and CsPbI$_3$ NCs retained the cubic morphology of the parent CsPbBr$_3$ NCs (Fig. 3a-c). High resolution TEM (HRTEM) image of single CsPbI$_3$ NC in Fig.3d clearly indicates the high crystalline nature of the exchanged NCs. However, all the three samples have different thickness as deduced from the different contrast in the TEM images. CsPbI$_3$ NCs were thicker than the original CsPbBr$_3$ NCs, whereas CsPbCl$_3$ NCs were thinner than the CsPbBr$_3$ NCs. This is consistent with the XRD observation, where growing along (200) plane direction can increase the thickness of the NCs

(Fig. S1). The elemental composition of the exchanged samples were obtained using energy dispersive X-ray spectroscopy (EDS). EDS data obtained from three different locations suggest the complete conversion of Br$^-$ to I$^-$ (Table S1).
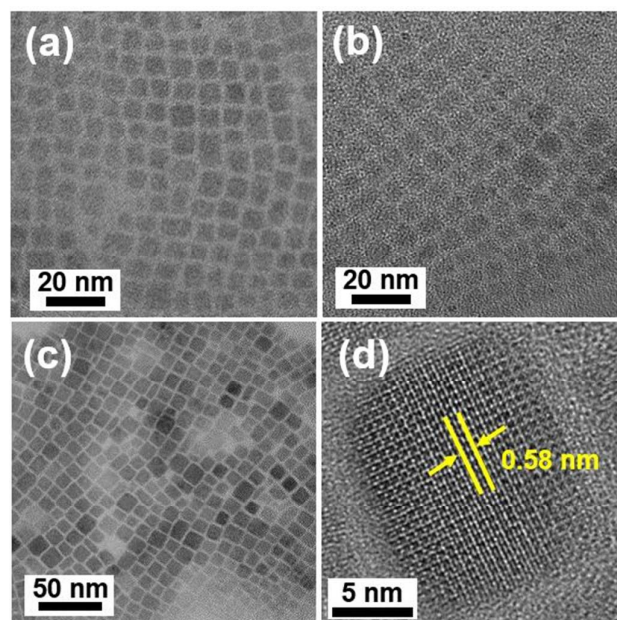

Fig. 3 TEM images of parent (a) CsPbBr$_3$ NCs and halide exchange synthesized (b) CsPbCl$_3$ and (c) CsPbI$_3$ NCs. HRTEM image of single CsPbI$_3$ NCs.

The halide exchange reactions of CsPbBr$_3$ to CsPbI$_3$ with different concentrations of LiI was monitored using absorbance and photoluminescence spectroscopy. The as-synthesized CsPbBr$_3$ has an absorbance peak around 485 nm which is red shifted to 510 nm after reacting with 10 μL of 0.16 M LiI (Fig. 4b). With increasing concentration of LiI, the absorbance peak gradually red shifts and reached a final value of 634 nm for 1.28 M LiI. This shift correlates with the XRD measurements, which shows a gradual shift of the (200) plane towards lower angles, suggesting the substitution of I$^-$ for Br$^-$ (Fig. 1b). As shown in Fig. 4c, the PL peak can be tuned from 508 to 654 nm with different concentrations of LiI. When LiI was replaced with LiCl, the absorbance and luminescence peaks of CsPbBr$_3$ were blue shifted to lower wavelengths. This is due to the gradual conversion of CsPbBr$_3$ to CsPbCl$_3$. The CsPbCl$_3$ NCs exhibited strong absorbance and narrow luminescence peaks (FWHM = 15 nm). The position of absorption and emission peaks of CsPbBr$_3$ NCs treated with different concentration of lithium halides are listed in Table S2. Time resolved photoluminescence decays of the CsPbX$_3$ NCs showed radiative lifetimes in the range of 1-16 ns with longer lifetime for iodide exchanged NCs (Fig. S2).
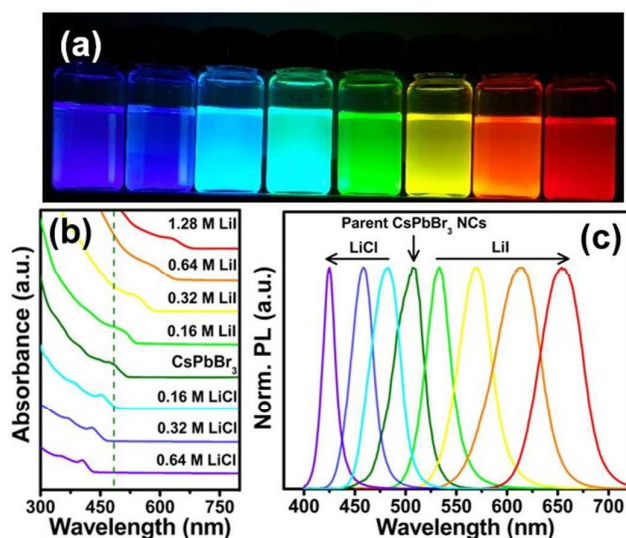
Fig. 4 (a) Digital photograph of anion exchange synthesized colloidal NCs in hexane under UV lamp (λ = 365 nm). (b) UV-vis absorption and (c) photoluminescence spectra of CsPbBr$_3$ NCs exchanged with different concentrations of LiI and LiCl.

Another interesting finding of our work is the reversibility of the anion exchange reactions. Once exchanged from CsPbBr$_3$ to CsPbI$_3$, the CsPbI$_3$ NCs can be reversed back to CsPbBr$_3$ by reacting with LiBr. Fig. S3a shows the absorption spectra of the reverse anion exchange reaction of CsPbI$_3$ NCs with different concentration of LiBr. The absorption peak of CsPbI$_3$ gradually blue shifted to the lower wavelength and reached a final value of 501 nm, which is in between the pure CsPbBr$_3$ NCs (485 nm) and slightly iodide exchanged CsPbBr$_{3-x}$I$_x$ NCs (510 nm). This suggests that the complete reversal to CsPbBr$_3$ is not possible. The corresponding PL spectra is shown in Fig. S3b. In a similar way, CsPbCl$_3$ NCs also can be reversed back to CsPbBr$_3$ using LiBr (Fig. S3c and d). The PL life time of the reverse exchanged sample did not change much compared with forward anion exchanged samples (Fig. S4). The morphology of the NCs remained unaltered after reverse exchange reactions (Fig. S5). We also found that a maximum number of five complete halide exchange cycles (*i.e.* Green to Red and Red to Green) possible for the same NCs solution (Fig. S6). After 5 cycles the nanocrystals are precipitated due to the increased concentration of ethanol in the solution.

In order to demonstrate the potential application of these NCs in optoelectronics, we fabricated photodectors devices with CsPbI$_3$ NCs film. We chose red emitting CsPbI$_3$ NCs since it has relatively longer radiative lifetime than the green and blue emitting ones. Longer radiative lifetimes could be beneficial in producing large photocurrents. The schematic of the photodetector is shown in Fig. 5a. CsPbI$_3$ NCs were drop casted on a heavily doped Si substrate with pre-patterned gold electrodes and annealed at 200 °C for 30 min in N$_2$ atmosphere. Annealing did not induce any change in the composition of the CsPbI$_3$ NCs as deduced from the XRD

patterns shown in Fig. S7. To illustrate the photoresponse of close-packed CsPbI$_3$ NC films, two-probe I-V was measured in the dark and under illumination using a laser diode at 405 nm as a function of incident light intensity. As shown in Fig. 5b, the photocurrent (I_{ph}), I_{ph} = I_{light} - I_{dark}, was increased by several orders of magnitude with increasing light intensity from 0.01mW/cm^2 to 1.38mW/cm^2, since the number of photogenerated carriers are proportional to the absorbed photon flux. Photosensitivity, which is defined as the ratio of photocurrent to the dark current (I_{ph}/I_{dark}), was exceedingly good (10^5).
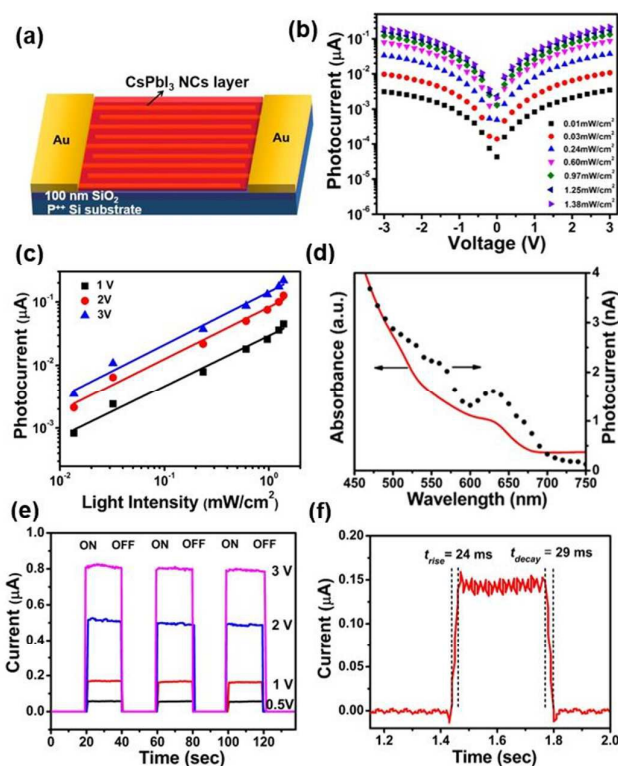

Fig. 5 (a) Schematic of the CsPbI$_3$ NCs photodetector (L=3μm, W=7800μm). (b) I-V characteristics of close-packed CsPbI$_3$ NC films as a function of incident light intensity. (c) Dependence of the photocurrent on the light intensity at different applied bias. (d) Absorption and spectral dependence of the photocurrent measured at 1V bias. (e) photocurrent-time (I_{ph}-t) response measured in the dark and under illumination using a laser diode at 405nm as a function of applied bias at fixed light intensity (P_{in}=1.98mW/cm^2). (f) Rise and decay time of the photodetector device.

The dependence of the photocurrents on light intensity is plotted as log-log plot in Fig. 5c. This can be fitted to a power law, $I_{ph} \sim P^{\alpha}$, where α determines the response of the photocurrent to the light intensity. The fitting gives a sublinear behavior with α = 0.8 which is consistent with different applied bias. The non-unity (0.5<α<1) exponent is a result of the complex process of electron-hole generation, recombination, and trapping within a semiconductor.[22] As shown in Fig. 5d,

the spectral response of the photocurrent was closely followed by the absorption spectrum of $CsPbI_3$ (λ=630nm) NCs, indicating the photocurrent is highly sensitive to the wavelength of illuminated light, and originate from the direct band-gap transition.

Fig. 5e shows photocurrent-time (I_{ph}-t) response measured in the dark and under illumination using a laser diode at 405 nm as a function of applied bias at fixed light intensity (P_{in}=1.98mW/cm^2). Upon the laser is turned on, the photocurrent is sharply increased with applied bias voltage due to the increase in carrier drift velocity. The devices were prompt in generating photocurrent with reproducible response to ON-OFF cycles. From the I_{ph}-t curves, we have noticed that sharp fall in photocurrent to dark current upon turned off the laser irradiation, which can reflect the capacitive response of the states at the NC surface. In addition, our photodetector exhibited relatively fast rise (t_{rise}=24 ms) and decay times (t_{decay}=29 ms) (Fig. 5f).

In summary, we have presented a simple and efficient method for halide exchange reactions in $CsPbX_3$ NCs. The exchange reactions proceed strikingly fast and complete within seconds at room temperature. The emission wavelength of any $CsPbX_3$ NCs can be tuned over the entire visible spectral range. Photodetectors fabricated from $CsPbI_3$ NCs were exhibited good on/off photocurrent ratio of 10^5 and rise and decay times of 24 and 29 ms, respectively.

Notes and references

1   M. A. Green, A. Ho-Baillie and H. J. Snaith, *Nat. Photon.,* 2014, **8**, 506.
2   W. S. Yang, J. H. Noh, N. J. Jeon, Y. C. Kim, S. Ryu, J. Seo and S. I. Seok, *Science,* 2015, **348**, 1234.
3   N. Ahn, D.-Y. Son, I.-H. Jang, S. M. Kang, M. Choi and N.-G. Park, *J. Am. Chem. Soc.,* 2015, **137**, 8696.
4   J. Luo, J.-H. Im, M. T. Mayer, M. Schreier, M. K. Nazeeruddin, N.-G. Park, S. D. Tilley, H. J. Fan and M. Grätzel, *Science,* 2014, **345**, 1593.
5   Gurudayal, D. Sabba, M. H. Kumar, L. H. Wong, J. Barber, M. Grätzel and N. Mathews, *Nano Lett.,* 2015, **15**, 3833.
6   Z.-K. Tan, R. S. Moghaddam, M. L. Lai, P. Docampo, R. Higler, F. Deschler, M. Price, A. Sadhanala, L. M. Pazos, D. Credgington, F. Hanusch, T. Bein, H. J. Snaith and R. H. Friend, *Nat. Nano.,* 2014, **9**, 687.
7   G. Li, Z.-K. Tan, D. Di, M. L. Lai, L. Jiang, J. H.-W. Lim, R. H. Friend and N. C. Greenham, *Nano Lett.,* 2015, **15**, 2640.
8   L. Dou, Y. Yang, J. You, Z. Hong, W.-H. Chang, G. Li and Y. Yang, *Nat. Commun.*, 2014, **5**, 5404.
9   B. R. Sutherland, A. K. Johnston, A. H. Ip, J. Xu, V. Adinolfi, P. Kanjanaboos and E. H. Sargent, *ACS Photonics*, 2015, **2**, 1117.
10 D. M. Jang, K. Park, D. H. Kim, J. Park, F. Shojaei, H. S. Kang, J.-P. Ahn, J. W. Lee and J. K. Song, *Nano Lett.*, 2015, **15**, 5191.
11 Chung, B. Lee, J. He, R. P. H. Chang and M. G. Kanatzidis, *Nature,* 2012, **485**, 486.
12 M. Kulbak, D. Cahen, G. Hodes and *J. Phys. Chem. Lett.,* 2015, **6**, 2452.
13 Chung, J.-H. Song, J. Im, J. Androulakis, C. D. Malliakas, H. Li, A. J. Freeman, J. T. Kenney and M. G. Kanatzidis, *J. Am. Chem. Soc.,* 2012, **134**, 8579.
14 C. C. Stoumpos, C. D. Malliakas, J. A. Peters, Z. Liu, M. Sebastian, J. Im, T. C. Chasapis, A. C. Wibowo, D. Y. Chung, A. J. Freeman, B. W. Wessels and M. G. Kanatzidis, *Cryst. Growth Des.,* 2013, **13**, 2722.
15 S.-i. Kondo, M. Kakuchi, A. Masaki and T. Saito, *J. Phys. Soc. Jpn.,* 2003, **72**, 1789.
16 L. Protesescu, S. Yakunin, M. I. Bodnarchuk, F. Krieg, R. Caputo, C. H. Hendon, R. X. Yang, A. Walsh and M. V. Kovalenko, *Nano Lett.,* 2015, **15**, 3692.
17 S. Yakunin, L. Protesescu, F. Krieg, M. I. Bodnarchuk, G. Nedelcu, M. Humer, G. De Luca, M. Fiebig, W. Heiss and M. V. Kovalenko, *Nat. Commun*., 2015, **6**, 8056.
18 Y. Wang, X. Li, J. Song, L. Xiao, H. Zeng and H. Sun, *Adv. Mater.*, 2015, **27**, 7101.
19 J. Song, J. Li, X. Li, L. Xu, Y. Dong and H. Zeng, *Adv. Mater.*, 2015, **27**, 7162.
20 G. Nedelcu, L. Protesescu, S. Yakunin, M. I. Bodnarchuk, M. J. Grotevent and M. V. Kovalenko, *Nano Letters*., 2015, **15**, 5635.
21 Q. A. Akkerman, V. D'Innocenzo, S. Accornero, A. Scarpellini, A. Petrozza, M. Prato and L. Manna, *J. Am. Chem. Soc.*, 2015, **137**, 10276.
22 H. Kind, H. Yan, B. Messer, M. Law, P. Yang, *Adv. Mater.,* 2002, **14**, 158.